

PROCEEDINGS OF SPIE

[SPIDigitalLibrary.org/conference-proceedings-of-spie](https://spiedigitallibrary.org/conference-proceedings-of-spie)

Interference wedged structures as light beam splitting elements

Margarita Deneva, Marin Nenchev, Elena Stoykova

Margarita Deneva, Marin Nenchev, Elena Stoykova, "Interference wedged structures as light beam splitting elements," Proc. SPIE 11047, 20th International Conference and School on Quantum Electronics: Laser Physics and Applications, 110471G (29 January 2019); doi: 10.1117/12.2516696

SPIE.

Event: International Conference and School on Quantum Electronics "Laser Physics and Applications": ICSQE 2018, 2018, Nessebar, Bulgaria

Interference wedged structures as light beam splitting elements

Margarita Deneva*^a, Marin Nenchev^a, Elena Stoykova^b

^a Technical University –Sofia and Plovdiv Branch, QOEL - Scientific Laboratory and Department of Laser Engineering, 4000 Plovdiv, Bulgaria; ^b Institute of Optical Materials and Technologies, Bulgarian Academy of Sciences, Acad. G. Bonchev Str., Bl.109, 1113 Sofia, Bulgaria

ABSTRACT

Based on our experience in the field of the interferential wedge, we present a new competitive application of such optical elements and structures built from them with theoretical description and experimental verification. We have demonstrated that a conventional interferential wedge or a structure of two wedges in compact layered implementation can be used as an attractive simple light power splitting element for a spatially and spectrally narrow light beam (basically a laser beam). The element can provide: 1) precisely and variably controlled ratio of the reflected and transmitted power by simple sliding in its plane of the list-like wedged structure with an apex angle of $\sim 10^{-5}$ rad; 2) division practically without energy losses; 3) power ratio control without causing change of propagation direction of the reflected and the transmitted beams that is of essential interest for applications in optical schemes with complex geometry of the beams propagation; no optical properties variation of the reflective layers (mirrors) during the sliding; 4) working at beam power densities of MW/cm² - GW /cm² when the optical element is built from optical materials (layers) with high light damage resistivity.

Keywords: interference wedge structure, light beam controlled splitting, compact dielectric layer realization

1. INTRODUCTION

In the present paper, we demonstrate both by theory and experiment that an Interference Wedged Structure (IWS) can be used for development of a simple optical element for light power splitting under illumination with a spatially and spectrally narrow light beam. The general property of the IWS is a variable thickness along its arms that leads to variation of the interference conditions of the partial waves within the structure and to a change in transmission and reflection respectively. The simplest representative of the IWS is the Interference Wedge (IW) with applications in laser technology, spectral analysis and optical metrology¹⁻¹⁰. Traditionally, it consists of two reflecting flat surfaces at a small angle between them. The wedge gap can be an air, a gas or a solid wedged layer. The apex angle, reflectivity of the surface coatings and refractive index of the layer between them form a unique fringe pattern in reflection and transmission when the IW is illuminated by spatially and temporarily coherent light^{1,11-13}. Under illumination with a monochromatic plane wave, the IW forms a sequence of transmission peaks, the so called Fizeau lines, along its rear surface. The spatial distance between these peaks is determined by the wedge angle and the wavelength of the illuminating light. The change of the wavelength shifts linearly the peaks position along the wedge and this makes possible the IW usage for spectral analysis of wide collimated beams. The free spectral range of the IW and the spectral resolution depend on the thickness of the wedge. At a given distance between Fizeau lines, the free spectral range decreases with the thickness whereas the spectral resolution given by the spectral width of the transmitted peak increases with the thickness. To make use of the wide spectral range of a thin IW and the high spatial resolution of a thick wedge, recently we proposed a new optical element built from a thin and a thick IWs with properly chosen apex angles and thicknesses. Both wedges form a compact interferential wedge structure – Composed Tunable Interference Wedged Structure (CTIWS)¹⁴⁻¹⁵ and demonstrate coincidence of a single transmission peak in the sequences of Fizeau lines along their rear surfaces.

As it is widely discussed in the literature, the light splitting elements are important as basic elements for a variety of scientific and industrial applications. The detailed review of the existing and currently used types of light beam splitters

* mar.deneva@abv.bg

as a cube beam-splitter, a pellicle beam-splitter, a polka dot beam-splitter and others is made in Ref. 16. Each type has its advantages and limitations.

For the group based on polarization splitting, in particular for cube beam splitters and splitters with a glass plate combined with a rotator of polarization, the drawbacks are the work with the polarized light, complexity, non-compactness and change in the reflected and transmitted beam positions for the angularly rotated polarizing glass plate. For the known coating plate splitters, the problems arise from the fixed splitting ratio and from high losses for the case of metallic coated plate. For the multi dielectric filters, the essential problem is the non-tunability; for the type based on the Fabry-Perot interferometer the change in the direction of the reflected and transmitted beams when varying transmittance by rotation of the element and also the required change in reflectivity of the mirrors are serious issues. For the type of the waveguide splitters and the micro-optics splitters, the problem is the control of the transmitted power and the tunability. Thus, any type of the existing splitters is suitable for some applications but presents disadvantages for the general use. This explains why development of a new type of splitters continues to be a field of active research¹⁷.

We consider the IWS implemented as an IW or a CTIWS, both realized in a compact layered design as a list-like wedged structure (apex angle of the gaps $\sim 10^{-5}$ rad), for development of a light power splitting element. We show that this element exhibits useful properties as follows: i) smoothly controllable variation of the ratio between the reflected and transmitted power at simple sliding; ii) power ratio control without causing change of propagation direction of the reflected and the transmitted beams (the latter is the desired option in optical schemes with complex geometry of the beams propagation); iii) negligible energy losses. The splitter can work at different wavelength within a large spectral range, e.g. from 0.5 to 0.8 μm and larger. In addition, when the IWS is built from optical materials (layers) with high light damage resistivity, the split beam power densities can be MW/cm^2 - GW/cm^2 . The element is compact with thickness of five to a few hundred micrometers on the transparent support; the dimensions with the support are $0.2 \text{ cm} \times 2 \text{ cm} \times 5 \text{ cm}$.

2. TRANSMISSION PROPERTIES OF INTERFERENTIAL WEDGED STRUCTURES

2.1 Transmission versus a wavelength

A conventional IW is schematically depicted in Fig.1. The wedge consists of two reflecting surfaces inclined at a small angle α_w , which is of the order of tens of micro-radians. The reflectivity of the coatings is higher than 50%, and this leads to dealing with multiple beams interference. The gap size between the reflecting surfaces is constant along the wedge ridge and increases linearly normally to the ridge. We consider beams falling normally to the ridge, and this makes the task one-dimensional. Under illumination with a plane wave at wavelength, λ , the IW forms a sequence of transmission peaks in the observation plane behind the wedge. The peaks are known as Fizeau lines, and the spatial separation between them along the X-axis is determined by the wedge apex angle α_w and the wavelength as $\Delta X = 0.5\alpha_w / \lambda$ for an air-gap IW. The separation remains the same along the whole IW's surface, but the resonant conditions for achieving a peak in transmission change with the wedge thickness. This leads to different behavior of thin and thick wedges in the spectral domain. The thin wedges demonstrate spectrally wide transmission (low spectral resolution) and large distance between the resonances (free spectral range) along the wavelength axis. The spectral resolution of thick wedges is high but the free spectral range substantially decreases.

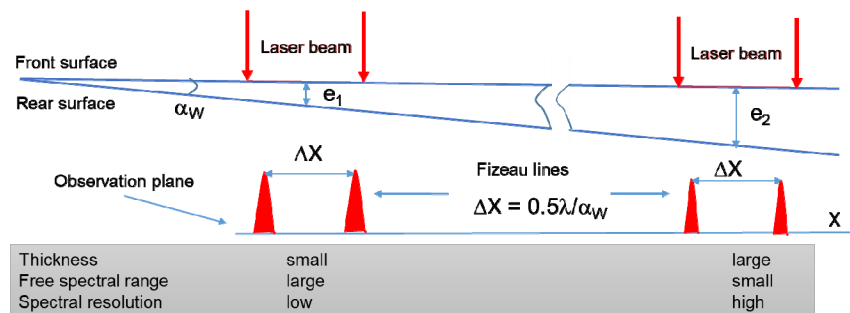


Figure 1. Schematic representation of the different optical behavior of Fizeau IW when the laser beam falls on sections with small and large thickness.

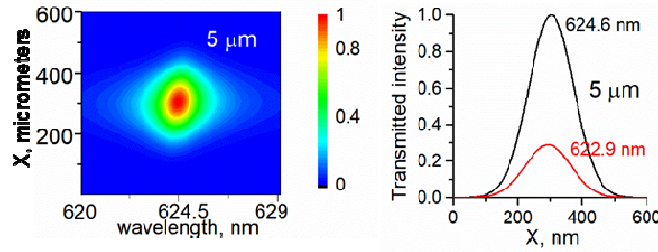


Figure 2. *Left*: contour map of transmitted intensity versus the wavelength for a 5 μm IW with an apex angle 5×10^{-5} rad and reflectivity of the coatings $R = 0.85$ for illumination with a Gaussian beam $I(x) = \exp[-(3-x/w_0)^2]$ at $w_0 = 100 \mu\text{m}$; *right*: intensity profiles at resonant wavelength 624.6 nm and far from the resonance at 622.9 nm.

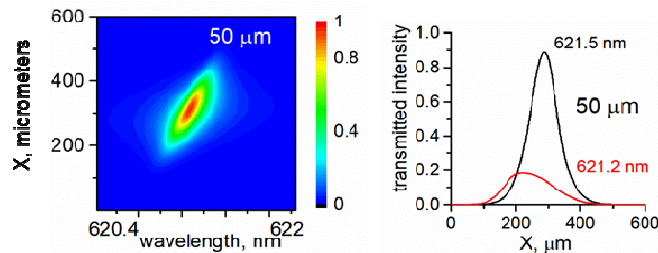


Figure 3. *Left*: contour map of transmitted intensity versus the wavelength for a 50 μm IW with an apex angle 5×10^{-5} rad and reflectivity of the coatings $R = 0.85$ for illumination with a Gaussian beam $I(x) = \exp[-(3-x/w_0)^2]$ at $w_0 = 100 \mu\text{m}$; *right*: intensity profiles at resonant wavelength 621.5 nm and far from the resonance at 622.9 nm.

Consequently, under illumination with a spatially narrow beam, the wedge transmission depends not only on the apex angle, reflectivity and the wavelength but also on the wedge thickness and the spatial width of the beam. For spatially narrow beams, the IW acts as a beam splitter which forms two beams - a reflected beam and a transmitted beam - at negligible energy loss. The ratio between the transmitted power and the power of the incident beam varies with the wavelength at a fixed position of the IW. It reaches maximum at a certain resonant wavelength. We compare in Fig. 2 and Fig. 3 transmitted intensity profiles formed by two air-gap wedges with one and the same apex angle 5×10^{-5} rad and reflectivity $R = 0.85$ but with thicknesses at the beam impact area correspondingly 5 and 50 μm . The IWs are illuminated quasi-normally by a Gaussian beam with intensity distribution, $I(x) = \exp[-(3-x/w_0)^2]$. The calculation starts from $x = 0$ and the size of the beam impact area on the IW surface is equal to $6w_0$. For calculation of the transmitted fringe pattern $I_T(x, \lambda)$ in the observation plane, we used approaches developed by us in ¹¹⁻¹³. As it can be seen, variation of the wavelength changes resonant conditions within the impact area of the beam on the wedge surface. The transmitted power increases up to the resonant wavelength and then goes down. The profiles formed by the thin IW are symmetrical with respect to the axis of the falling beam. For the thick wedge, the resonant profile is symmetrical with respect to this axis whereas the peaks formed at wavelengths lower or higher than the resonant wavelength are asymmetrical with their maxima located to the left and to the right of the falling beam axis.

The dependence of the normalized transmitted power

$$\rho(\lambda) = \frac{\int_{-\infty}^{\infty} I_T(x, \lambda) dx}{\int_{-\infty}^{\infty} I(x) dx} \quad (1)$$

on the wavelength characterizes the spectral resolution. The spectral curves, $\rho(\lambda)$, are shown in Fig. 4 for three wedges with the same apex angle and reflectivity of the coatings. The obtained transmission spectral widths defined as full widths at half maximum and the free spectral range for these IWs are given in Table 1. We see that the three wedges show completely different parameters in transmission although they are characterized by the same separation of Fizeau

lines. The important fact is that the curve $\rho(\lambda)$ contains rather long sections of linear increase/decrease of the transmitted power as a function of the wavelength.

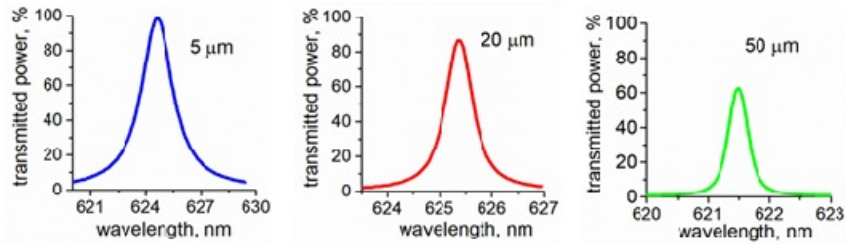


Figure 4. Transmitted power (given as a percentage of the incident beam power) as a function of the wavelength for three IWs with thickness 5, 20 and 50 μm , apex angle 5×10^{-5} rad and reflectivity of the coatings $R = 0.85$ for illumination with a Gaussian beam $I(x) = \exp[-(3-x/w_0)^2]$ at $w_0 = 100 \mu\text{m}$. Table 1. Spectral width $\delta\lambda$ and the free spectral range $\Delta\lambda$ as a function of the IW thickness

e	5 μm	20 μm	50 μm
$\delta\lambda$, nm	1.38	0.34	0.14
$\Delta\lambda$, nm	40	10	4

2.2 Transmission control by wedge translation

The obtained curves of the transmitted power show that one can control the IW's transmission for a narrow monochromatic beam in a wide range. At a given wavelength, this can be done by wedge translation in the plane of its front surface (parallel to X axis in Fig.1). Shifting the wedge along the X axis changes the resonant conditions and produces variation of the transmitted power similar to that described by the spectral curves in Fig. 4. The power variation

in this case is given by $\rho(e_i + \Delta e) = \frac{\int_{-\infty}^{\infty} I_T(x, e_i + \Delta e, \lambda) dx}{\int_{-\infty}^{\infty} I(x) dx}$ where e_i is the initial thickness corresponding to the

leftmost point of the incident beam impact area at $x = 0$ on the wedge surface and Δe is the thickness increment due to the wedge translation. An equal shift along the X axis results in different decrease of the transmitted power in the case of thin and thick wedges due to different resonant conditions formed on their surfaces. To prove that an IW can be used as a splitter with a controllable ratio between the powers of the transmitted and the reflected beams, we made numerical simulation of propagation of a Gaussian beam through three wedges with thicknesses 5, 20 and 50 μm . The obtained functional form of $\rho(e_i + \Delta e)$ is the same as that of $\rho(\lambda)$. As it is possible to find for all three wedges a large section in $\rho(e_i + \Delta e)$ with linear increase (or decrease) of power, linear power control of the transmitted beam by sliding the IW is feasible at high precision for a large range of ratios $\rho(e_i + \Delta e)$ between the transmitted and incident power. The slope of the linear section is the smallest for the 5 μm wedge and the largest for the 50 μm wedge. The largest linear variation of $\rho(e_i + \Delta e)$ is observed for the 5 μm wedge.

Thus, the thin wedge provides the easiest way to control the transmitted power within the largest possible range but at the expense of low spectral resolution. The higher spectral resolution of the thick wedge is contra-balanced by the small free spectral range. The IW spectral performance can be improved by combining two IWs with different parameters. If two wedges are characterized with the same ratio α_w/e where e is the IW thickness, it is possible to ensure synchronous increase (or decrease) of the power transmitted through both wedges by producing the same shift along X axis. In such a way, these two wedges can form an IWS with controllable transmission. To prove this statement, we made numerical experiment with three IWs with thicknesses 5, 20 and 50 μm . All wedges had reflectivity of the coatings $R = 0.85$, and the apex angles were chosen to be 1.25×10^{-5} rad, 5×10^{-5} rad and 12.5×10^{-5} rad. The wavelength was equal to 616.5 nm. We calculated the transmission for the three wedges by shifting at regular intervals the leftmost point of the beam impact area on the wedge surface. To observe coincidence of maximum resonant transmission for all three wedges at the same

shift value (equal in the simulation to 0.486 mm), we adjusted the wedge thickness e_i at a zero shift to be 5.454 μm , 20 μm and 50.145 μm respectively for the used IWs. In the experiment, coincidence of the resonant maxima can be achieved along the spatial and spectral axes by sliding the one of the wedges with respect to the other. We made calculations for shifting the IWs up to 0.5 mm. The obtained transmitted intensity profiles for all shifts are shown in Fig.5. The sections of the curve $\rho(e_i + \Delta e)$ for the three wedges for applying shifts within 0.5 mm along X are shown in Fig. 6. The maximum transmission for all wedges is observed at a shift of 0.486 mm. Transmission falls from 98% to 60% for the 5 μm IW at a shift of 0.5 mm whereas for the 50 μm IW such a shift leads to practically zero transmission. An IWS formed from these two wedges is characterized with an enlarged free spectral range and the spectral resolution of the thick wedge. However, the power control range is given also by the thick wedge.

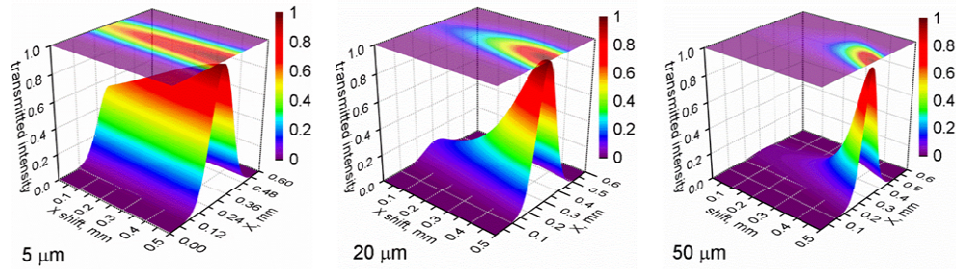


Figure 5. Distributions of transmitted intensity at a wavelength 616.5 nm as a function of the IW's shift along X axis in the plane of its front surface; parameters of the IWs are: $e_1 = 5 \mu\text{m}$, $\alpha_{W1} = 5 \times 10^{-5}$ rad; $e_2 = 20 \mu\text{m}$, $\alpha_{2W2} = 5 \times 10^{-5}$ rad; $e_3 = 50 \mu\text{m}$, $\alpha_{W3} = 12.5 \times 10^{-5}$ rad; reflectivity of the coatings $R = 0.85$ for illumination with a Gaussian beam $I(x) = \exp\left[-(3-x/w_0)^2\right]$ at $w_0 = 100 \mu\text{m}$.

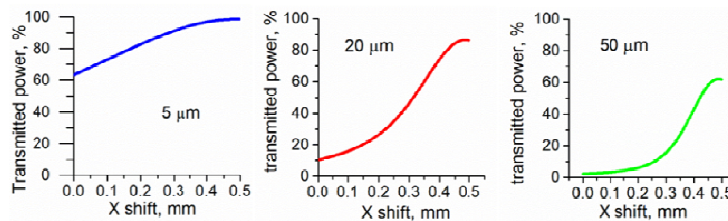


Figure 6. Transmitted power (given as a percentage of the incident beam power) at a wavelength 616.5 nm as a function of the IW's shift along X axis in the plane of its front surface; parameters of the IWs are: $e_1 = 5 \mu\text{m}$, $\alpha_{W1} = 5 \times 10^{-5}$ rad; $e_2 = 20 \mu\text{m}$, $\alpha_{2W2} = 5 \times 10^{-5}$ rad; $e_3 = 50 \mu\text{m}$, $\alpha_{W3} = 12.5 \times 10^{-5}$ rad; reflectivity of the coatings $R = 0.85$ for illumination with a Gaussian beam $I(x) = \exp\left[-(3-x/w_0)^2\right]$ at $w_0 = 100 \mu\text{m}$.

3. EXPERIMENTAL INVESTIGATIONS

According the discussion in the theoretical part, the principle of the proposed power and spatial splitting of an incident monochromatic beam can be formulated as follows: utilization of the IWS's transmission dependence on the distance from the position corresponding to the wedged structure transmission resonance. From our experimental observations and their physical comprehension, we have developed two ways to do the splitting. The first approach is related to splitting of a collimated small diameter laser beam. The second approach considers splitting after focusing the incident beam, which is of interest for fiber optics instrumentation and optical communications. The second approach permits also to split large diameter beams.

We studied splitting of collimated beams for beam diameters of 1-2 mm or a part of a millimeter, that are typical for the He-Ne, Argon, VICSEL, diode-pumped smaller Nd:YAG lasers etc. The principle of the two approaches is elucidated in

Fig7. The upper graph gives the calculated transmission T_{IWS} and reflection R_{IWS} of a single angle IWS following the methodology presented in ¹¹⁻¹³. The calculation is made at typical values of the parameters: $e_1 = 20 \mu\text{m}$, $\alpha_1 = 5 \cdot 10^{-5} \text{rad}$, $R = 0.85$, for $n_1=1$ and wavelength $\lambda = 632.8 \text{ nm}$ (He-Ne laser), the incident angle is 5° . The graphs at the bottom represent the same resonance for an extended scale of the X axis (along the wedge arm). Let's the laser beam falls at the resonant wavelength onto the position corresponding to the wedge resonance. The beam is with diameter 1 mm (we assume a Gaussian beam with a waist of 0.5 mm or homogeneous intensity distribution). This is shown with solid lines in the extended graphs. The beam is partially transmitted and partially reflected, i.e. it is split. At sliding the wedge, the beam impact area corresponds to a different thickness (dotted lines). As a result, the powers of the reflected and transmitted beams represent varying parts of the power of the incident beam. In the ideal case without absorption in the layers and parasitic reflections, the full incident power is divided between the two beams at a ratio controlled through changing the position of the beams with respect to the resonance maximum. The detailed calculation of the ratio as a function of the position is given below.

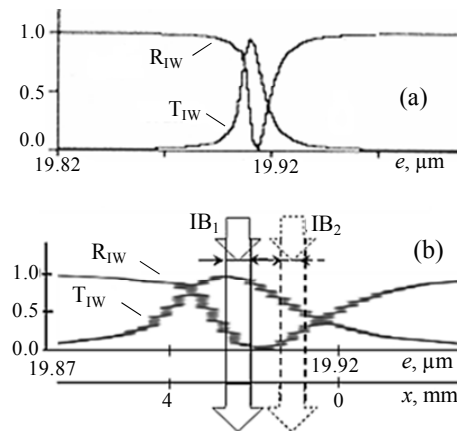


Figure 7. Simplified representation of the proposed approaches in the case of using an IWS (IW) for light beam splitting. (a) the calculated transmission (T_{IW}) and reflection (R_{IW}) for a single angle IWS (IW); (b) - the same resonance in an extended scale of X axis along the wedge arm.

Naturally, as it can be seen in Fig. 7, for a beam diameter smaller than the resonance spatial width (typically $\sim 1.5 \text{ mm}$), a small change of spatial distribution can be expected. The experimental examples are shown below. To obtain variable transmission for a large diameter collimated beam ($\sim 3\text{-}4 \text{ mm}$), one should use larger spatial or spectral resonance width, obtained at lower reflectivity of the mirrors or at smaller wedge structure thickness. As an example, Fig. 9 shows three graphs of the resonant transmission peak for the given above IW parameters at different reflectivity (0.85, 0.85 and 0.6). The calculations are performed for modeling the IWS as a sequence of Fabry-Perot interferometers with linearly increasing thickness. For a small IWS thickness in the range $1\text{-}50 \mu\text{m}$, wedge angles $10\text{-}100 \mu\text{rad}$, reflectivity of the mirrors smaller than 0.9 and incident angles less than 15° , the results provided by this model are in acceptable as they correspond well to precise calculations and experimental data and can be used for practical estimation. The graphs show the essential enlargement of the resonance spatial width for the low reflectivity and the possibility to vary the ratio discussed above without essential change of the transmitted and reflected beam profiles for large beams. The other solution is decreasing the IWS thickness to be smaller than $1\text{-}2 \mu\text{m}$ with very small wedge angle ($\sim 10^{-6} \text{ rad}$). However, such precision needs very high flatness of the optical support on which layers are superimposed.

For experimental study of the splitting, we used IWSs with the given above parameters at reflectivity of the mirrors equal to 0.8 and 0.65. The experimental arrangement and demonstration of splitting is illustrated in Fig. 8.

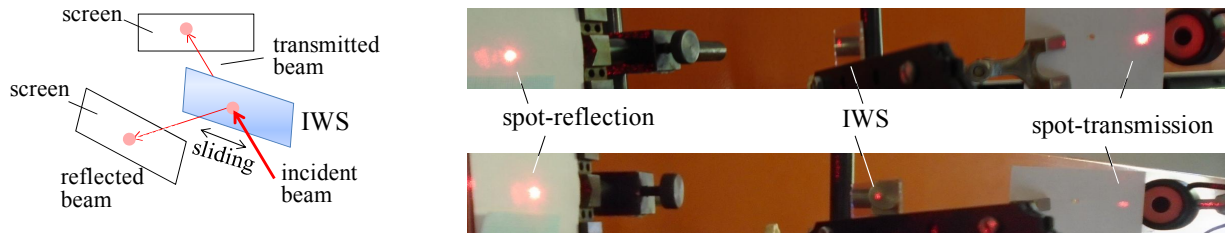


Figure 8. *Left*: schematic of controllable splitting by sliding the IWS; *right*: the photograph demonstrating the realized splitting. The practical arrangement corresponds to the schematic in the left figure. The variation of the beam intensities can be seen in the photographs by the variation of the incident spot intensity.

The power of the incident laser beam for the system in Fig. 8 was 15.6 mW. The maximum transmitted power was 8.9 mW or $\approx 57\%$, and the reflected power was 5.4 mW or about 35%. The losses of approximately 8% can be related to the absorption in the gap-layer, layers of the mirrors and to Fresnel reflection from the non-layered side of the optical support. Theoretically for the ideal (lossless) layers and an AR optical support, the energy losses must be near zero. This is a goal that can be achieved by development of very high quality layers (lossless and with nano-homogeneity). The intensity distribution in the divided beams is also important. In general, the distribution must depend on the diameter of the incident beam and the place of incidence with respect to location corresponding to the resonant transmission. The experiment shows that for the small diameter beams compared to the spatial width of the resonance, i.e. about 1 mm for the typical wedge thickness, angle and $R \sim 0.8$, the transmitted spot for a homogeneous incident beam has near uniform distribution, slightly distorted on one side. As additional advantage of the splitting variation by sliding of the structure is preservation of the optical properties of the reflecting layers (mirrors) in contrast to the case when this is via rotation (as e.g. FP type rotated splitters). Typical computed graphs of the IWS transmission as a function of X for different reflectivity of the wedge mirrors R are plotted in Fig. 9. The evaluation shows that very convenient for employment of the IWS as a beam splitting element is its realization with low reflectivity mirrors ($\sim 60\%$). In the same figure (right), the experimentally measured curve of transmission for He-Ne laser beam ($\lambda = 632.8$ nm; Gaussian diameter of 1 mm) through an IW with given above parameters and reflectivity of 0.6 is presented. The analytical results and experiment show good agreement and confirm the made conclusion of making the splitting element at lower reflectivity. The left section of the curve shows a smooth variation of the transmitted power at the sliding movement of the IW. Also, the reflected and transmitted spots, as it can be seen in Fig. 8, have relatively circular shapes.

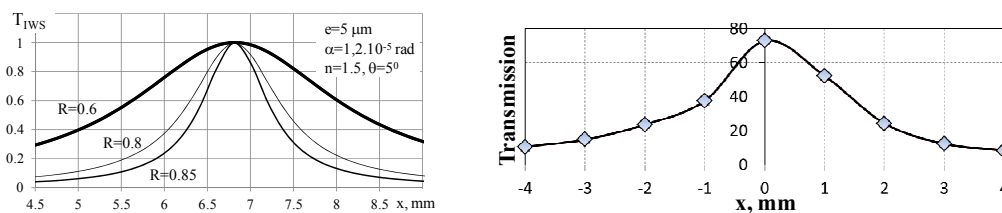


Figure 9. *Left*: calculated curves of IWS (IW) transmission resonances as function of X at different mirror reflectivity R . The parameters of IWS are given in the figure; *right*: typical experimentally measured curve of beam transmission of He-Ne laser beam ($\lambda = 632.8$ nm; Gaussian diameter of 0.7 mm) through an IW with given above parameters and the mirror reflectivity of 0.6.

The reflected and transmitted spot distortions expressed as appearance of a tail, as we have discussed in ⁴⁻⁶, are obtained for the high reflectivity mirrors ($R \sim 95-98\%$) at high thicknesses in the interval of 50-800 μm . However, such parameters are not suitable for using the IWS as a beam splitting element.

As a second issue we consider the splitting action of the IWS for a focused laser beam. The beam, focused to a spot of 100 – 400 μm in the experiment, has optical behavior similar to a collimated small diameter incident beam. We present in Fig. 10 the typical case of IWS action with focused Gaussian beam from He-Ne laser ($\lambda = 632.8$ nm, Gaussian diameter of 1 mm). The IWS in the figure is a wedge with the parameters, given in Fig.7. The focusing lens had a focal

length of 2 cm and was positioned at distance of 2 cm from the IWS. The angle of incidence was 5° . To visualize the reflected spot a tracing paper was used close to the lens.

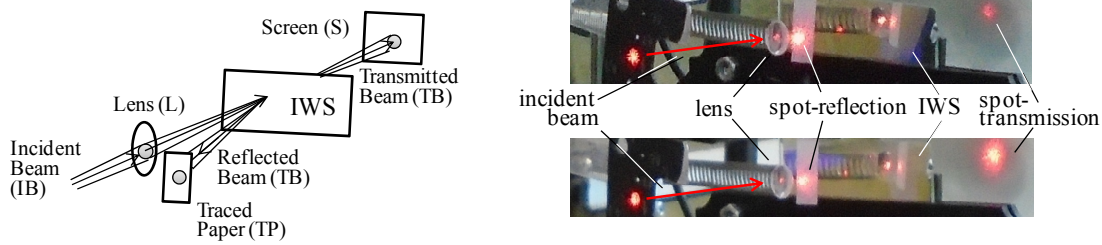


Figure 10. The schematic of illumination with a focused laser beam (*left*) and typical photographs (*right*) of splitting with focusing. A red He-Ne laser is used (632.8 nm).

The transmitted beam illuminated a white screen. Two cases are shown for illustration: the top photograph presents sliding of the IWS near the end of the spatial resonance and the bottom shows the result when the structure is sliding and the beam is inside the area of the resonance maximum. The splitting of the beam at ratios of 1/25 for the top picture and 15/4 for the bottom is measured. The typical power losses for some of the beams are about 10%. The spots on the screen show the Gaussian-like shape and divergence which corresponds to that of the incident focused beam ($\sim 10^\circ$). If it is necessary, by using two lenses for focusing, we can collimate the transmitted and reflected beams to obtain parallel beams or to focus each beam to a small point (~ 0.1 mm). We have found that for a focused divergent laser beam ($5\text{--}20^\circ$), the IWS presents the spectral and spatial selectivity similar to that for a small diameter (1-2 mm) parallel incident laser beam with the same resonances and transmission. This observation stimulated us for coupling the IWS with a $100\ \mu\text{m}$ fiber that is of interest for optical communication hardware. For direct illumination of the IWS by a fiber close to the structure, existence of spatial resonances at a distance, equal to that for a collimated laser beam illumination, is observed and also the transmission-reflection ratio is controlled by sliding as well. Such a case is presented in Fig. 11(a), where the IWS with parameters, given in Fig. 7, is illuminated with the $100\ \mu\text{m}$ fiber.

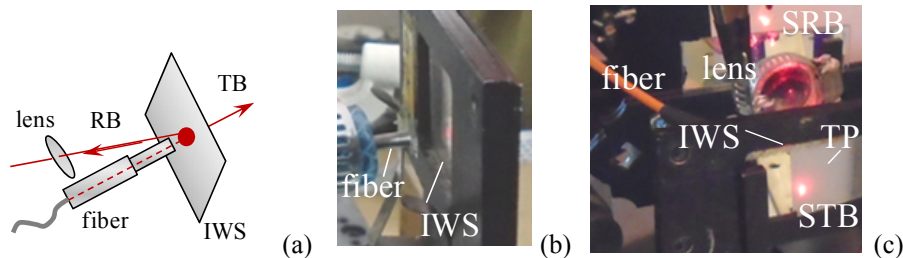


Figure 11. (a) Schematic of direct illumination of the IWS by a fiber close to the structure, the reflected beam is focused or collimated by lens (TB – transmitted beam, RB – reflected beam); (b) side view of the fiber; (c) the arrangement in action in the IWS resonance – for visualization the tracing paper TP is superimposed on the output side of the IWS, STB – the spot of the transmitted beam, SRB – the spot of the reflected beam that is focused by the lens on the screen (or in the other fiber).

Figure 12 (a) gives the transmission beam as a function of the distance from the exact resonance position for illumination with 1 mm diameter He-Ne laser beam (632.8 nm). We have estimated the angular dependence using the model, which represents the IWS as a sequence of Fabry-Perot interferometers with linearly variable thickness. The calculated curves of the angular dependence of the IWS transmission for parameters given in Fig. 7 are plotted in Fig.12(b). It can be seen that for relatively low reflectivity of the mirrors, the IWS transmits for large variation of the incident angle, i.e. for relatively large divergence of the illuminating beam what coincides with the experimental observation.

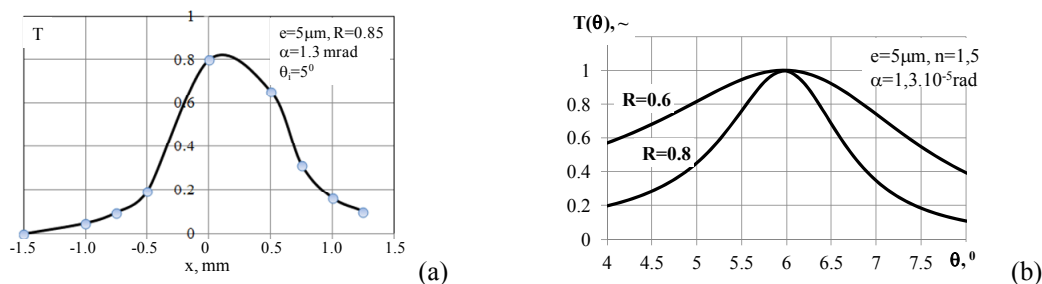


Figure 12. (a) The experimental curve of the IWS transmission (the IW parameters are given in Fig. 7) for illumination with tightly close 100 μm fiber; (b) - transmission as a function of the incident angle for different R .

The experimental study in this work was performed with CW lasers – a red and yellow He-Ne laser at 632.8 nm and 5941 nm and a green semiconductor laser. We obtained also preliminary results using a pulsed green Nd:YAG laser (532 nm, pulse duration 100-300 ns, low energy of the order of 1 mJ, repetition rate of 3 Hz). For these pulse lengths, no difference with respect to the results obtained with the described CW lasers, including focusing with a short focal distance lens, was observed. As a next step, we envisage conducting experiments with sub-nanosecond pulses. The arrangement of such a system has already started.

CONCLUSION

We have presented a new light beam splitting element, based on the Interference Wedged Structure. The developed beam splitter demonstrates properties which provide action competitive to existing splitters for many applications. A very important feature of the element is its compactness in view that it is realized as a list-like element with a micrometer thickness (the size with the support is 0.2 cm \times 2 cm \times 5 cm). It allows for precise and smooth controlling of the ratio between the reflected and transmitted power by simple sliding in the plane of the structure. Power division is realized practically without energy losses. The power ratio control is performed by keeping intact the directions of the reflected and the transmitted beams. The latter is of essential importance for optical arrangements with complex geometry that needs keeping unchanged directions of the beams. As addition, the variation by sliding does not change the optical properties of the consisting structure layers (mirrors). Tuning of the working wavelength is made in a simple way by sliding. Our results show that the splitter works well for the CW laser light and also for the pulsed laser light (the study was made up to 100 ns pulse length). In addition, the element can potentially work at beam power densities of MW/cm² - GW/cm², when optical layers are with high light damage resistivity. The element is especially competitive for the case of relatively narrow light beams with diameters from a millimeter to a few millimeters. Such beams are emitted by a variety of important light sources (He-Ne, Ar, He-Cd, Nd; YAG, semiconductors). We demonstrate also the operation with a focused laser beams that widens the limits of applicable beam diameters and permits utilization of the optical fiber setups and devices. The presented beam splitter enriches the elemental base of optics by being a component for useful devices in many applications.

Acknowledgement. This work was supported by Bulgarian Science Fund, project DN-17/7 “Elements and devices in optics and quantum electronics on the base of wedged interferential structures for laser technology, optoelectronics, optical communications, metrology and spectrum analysis.”

REFERENCES

- [1] Born, M., Wolf, E. [Principles of Optics], Cambridge University Press (1999).
- [2] Demtredner, W., [Laser spectroscopy], Springer, 4th Ed. (2008).
- [3] Nenchev, M.N., Meyer, Y.H., “Two-wavelength dye-laser operation using a reflecting Fizeau interferometer,” Appl. Phys. 24,7-9 (1981)
- [4] Nenchev, M.N., Meyer, Y.H., “Laser tuning with combined system of Interference wedges,” Proc. SPIE 473, 181 (1984)

- [5] Nenchev, M.N. ,”Two-wavelength laser oscillator,” IIR BG patent 41454 (26.02.1986).
- [6] Lee, L.S and Schawlow, A.L., “Multiple-wedge wavemeter for pulsed lasers,” Optics Letters 6 (12), 610-612 (1981).
- [7] Deneva, M., Uzunova, P., Nenchev, M., “Tunable subnanosecond laser pulse generation using an active mirror concept,” Opt. Quant. Electron. 27(39), 193-212 (2007).
- [8] Kajava, T. , Lauranto, H., Saloma, R., “Fizeau interferometer in spectral measurements,” J. Opt. Soc. Am. B10, 1980 – 1989 (1993).
- [9] Belmonte A., Lázaro, A., “ Measurement uncertainty analysis in incoherent Doppler lidars by a new scattering approach,” Opt. Express 14, 7699-7708 (2006).
- [10] Kumar, Y., Chatterjee, S., “Simultaneous measurement of refractive index and wedge angle of optical windows using Fizeau interferometry and a cyclic path optical configuration,” Appl.Opt. 48 (24), 4756-4761 (2009).
- [11] Nenchev, M., Stoykova, E., “Interference wedge properties relevant to laser applications: transmission and reflection of the restricted light beams,” Opt. Quant. Electron. 25, 789-799 (1993).
- [12] Stoykova, E., Nenchev, M., “Fizeau wedge with unequal mirrors for spectral control and coupling in a linear laser oscillator-amplifier system,” Appl. Optics. 40, 275402-5411 (2001).
- [13] Stoykova, E., Nenchev, M., “Gaussian Beam Interaction with Air-gap Fizeau Wedge,” J. Opt. Soc. Am. 27, 58-68 (2010).
- [14] Nenchev, M., Stoykova, E., Deneva, M., “Composite wavelength tunable wedged interference structures with increased free spectral range”, accepted for publication in Opt.Quant. Electron. (2018);
- [15] Nenchev, M., Deneva, M., Stoykova, E., “Wavelength division/multiplexing devices,” BG Patent reg. No 110967 (2017).
- [16] RP Photonics Encyclopedia, https://www.rp-photonics.com/beam_splitters.html
- [17] Turner, M.D., Saba, M., Zhang, Q., Cumming, B.P., Schröder-Turk, G.E., Gu, M., “Miniature chiral beamsplitter based on gyroid photonic crystals,” Nature Photonics 7, 801–805 (2013).